Paper No.
02545

CORROSION 2002

Comparison of Localized Corrosion of Fe-Ni-Cr-Mo Alloys in Chloride Solutions Using a Coupled Multielectrode Array Sensor

Lietai Yang, Narasi Sridhar and Gustavo Cragnolino
Center for Nuclear Waste Regulatory Analyses
Southwest Research Institute
6220 Culebra Road
San Antonio, TX 78238

ABSTRACT

A multielectrode localized corrosion sensor was developed and used for comparing localized corrosion of Fe-Ni-Cr-Mo alloys in chloride solutions. Experimental results indicated that the coupled multielectrode sensor provides a rapid real-time response to changes in temperature and salt concentration. It was demonstrated that the sensor has a lower detection limit of 5×10^{-11} A with respect to corrosion current and 2×10^{-8} A/cm^2 with respect to the corrosion current density for the miniature electrodes used in the sensors.

Key word: galvanically coupled sensor; multiple-electrode sensor; multielectrode; localized corrosion sensor; wire beam electrode; on-line localized corrosion monitoring.

INTRODUCTION

Because of its resistance to corrosion, alloy 22 has been selected by the U.S. Department of Energy as the candidate outer barrier material for the high level nuclear waste containers in the proposed geological repository[1] at Yucca Mountain, N.V. To adequately protect the public from exposure to radiation, the container is designed to last for many thousands of years, by which time, radioactivity would decay significantly[2]. As the life of the nuclear waste containers is estimated based on models that use parameters derived from relatively short-term experiments, continuous monitoring of corrosion rate after the repository closure is important to gain confidence in model estimates. As localized corrosion generally results in more rapid penetration of the material[3], the monitoring of localized corrosion is more important than monitoring of uniform corrosion. However, many of the effective on-line monitoring techniques such as the electrical resistance method[4-6] and the linear polarization method[7-8] are not adequately sensitive to localized corrosion. Electrochemical noise has been used for the measurement of pitting[9] and crevice corrosion[10]. Although it is a useful method to indicate the electrochemical activity

due to localized corrosion, it has been shown that there is no consistent dependence between the measured signals, such as the pitting index, and the localized corrosion rate[11,12]. This paper presents the results obtained during the evaluation of a coupled multiple-electrode sensor[13] as an in-situ online monitor for localized corrosion of proposed container materials.

EXPERIMENTS

The schematic diagram of the coupled multiple-electrode array sensor is given in Figure 1. It is similar to the Wire Beam Electrode used by Tan et al[14,15] except the coupling of the electrodes is through resistors which allow the use of a high resolution voltmeter instead of a zero resistance ammeter for the measurement of the coupled currents. The working principle of the sensor, the auto-switching and electrode-location-mapping instrument have been described previously[16]. The sensing electrodes were cut from 1-mm diameter wires of types 304 and 316 stainless steels (UNS S30400 and UNS S31600), and nickel based alloys 22, 276 and 600 (UNS N06022, UNS N10276 and UNS N06600). A 1010 carbon steel (UNS G10100) wire (1-mm diameter) was used as the sensing element in a comparative experiment. The chemical compositions of these metal wires are given in Table 1. The sensors were polished with 600 grit SiC paper prior to the start of the tests. All solutions were prepared using reagent chemicals and de-ionized water. Experiments were conducted in a 3-L glass cell, filled with 2-L air-saturated solutions. The solution was slowly agitated on a magnetic stir plate during the experiments.

RESULTS AND DISCUSSIONS

Figures 2 through 5 show typical responses of the currents measured from four coupled multiple electrode sensors made of alloys 22 and 600 and types 316 and 304 stainless steel to the changes of temperature in 0.1M ferric chloride solution. It has been shown from our previous work[16,17] that the standard deviation of the sensor currents is an effective single-parameter indicator for localized corrosion. The standard deviation of the currents for each sensor is also plotted in the corresponding figures. As shown in Figures 2 through 5, all sensors, with exception of the alloy 22 sensor, showed a significant increase in the standard deviation with the change from de-ionized water to ferric chloride solution. In addition, both the maximum anodic current (most negative currents) and the standard deviation of each sensor increased with increasing temperature. Figure 2 also shows that the sensor was able to detect the changes in standard deviation at levels as low as 5×10^{-11} A.

Figure 6 presents a direct comparison for the standard deviation signals from the four sensors. Figure 7 presents the standard deviations that were averaged over time for the four sensors as a function of temperature. For comparison, a data point obtained with a mild carbon steel sensor consisting of 24 electrodes (1 mm diameter) at 18°C is also included in Figure 7. As shown in Figures 6 and 7, the resistance of the metals to localized corrosion in the 0.1M ferric chloride solution at temperatures up to 60°C increases in the following order:

Carbon steel<alloy 600<type 304<type 316< alloy 22

Leaving aside the carbon steel, this order is consistent with the pitting resistance equivalent numbers (PRE) calculated according to the elemental composition of the alloys using the following formulas[18] (Table 2):

$$PRE = \%wt\ Cr + 3.3\ \%wt\ Mo + 20\ \%wt\ N \quad (1)$$

$$PRE' = \%wt\ Cr + 3.3\ (\%wt\ Mo + \%wt\ W) + 30\ \%wt\ N \quad (2)$$

$$PRE'' = \%at\ Cr + 3.3\ (\%at\ Mo + \%at\ W) + 30\ \%at\ N \quad (3)$$

Where %wt is the weight percent and %at is the atomic percent. Eq 1 has been commonly used for iron base alloys and Eqs 2 and 3 were proposed for nickel base alloys.

At 90°C, the resistance of alloy 600 becomes slightly better than that of type 304 stainless steel. As expected, the resistance of alloy 22 is far better (by more than 3 orders of magnitude) than that of the stainless steels and alloy 600.

Post test examination confirmed that the electrodes of the types 316 and type 304 stainless steel sensors were severely pitted (Figures 8 and 9) and the electrodes of the alloy 22 were slightly pitted (Figure 10).

Figures 11 and 12 show the responses of the standard deviations of the sensor currents and the open circuit potentials of the sensors to the changes in chloride concentration in the NaCl solution at room temperature. As shown in Figure 11, the standard deviations of the alloy 276 and types 316 and 304 stainless steel sensors increased with increasing chloride concentration. The standard deviation of the alloy 22 sensor was initially $3x10^{-9}$ A in de-ionized water immediately after it was polished, but decayed to the $5x10^{-11}$A over 3 days. After the sensor became passivated in the de-ionized water, it did not respond to the addition of chloride at concentration levels up to of 4 M. As shown in Figure 12, the open circuit potentials of the stainless steels and alloys also responded to the changes in chloride concentration well. Each time the chloride was added, the potentials of the metals became more negative.

In principle, the localized corrosion penetration rate may be estimated based the maximum anodic current of the sensor. Examples of the maximum anodic currents are the ones from the #4 electrode in Figure 2 during the time period when the temperature was 18°C and from the #6 electrode in Figure 5. As the directly measured maximum anodic current as shown in Figures 2 through 5 depends on the information from only one of the many measured values and therefore has a greater uncertainty, statistical methods may be used to derive the maximum anodic current using the information from all the electrodes. According to our previous analyses[16,17], the maximum anodic current for the coupled multielectrode sensor, I_{max}, may be estimated by:

$$I_{max} = 3\sigma \quad (4)$$

where σ is the standard deviation of the distribution of the maximum current from each of the sensors. A penetration rate may be calculated from the maximum current density through Faraday's law. However, such a calculation currently not possible because it requires the assessment of the actual dimension and area of the pits within the most corroded electrode and the understanding of the distribution of the corrosion current between the internal and the external circuits. Figure 13 shows the apparent maximum anodic current densities, obtained using Eq 4 and the apparent surface area ($0.1^2\pi/4=0.00785$ cm^2), for the various sensors in $FeCl_3$ solution as a function of the reciprocal of temperature. As shown in Figure 13, the apparent maximum anodic currents of the types 304 and 316 stainless steel and alloy 600 sensors are exponentially related to the reciprocal of temperature. For alloy 22, the apparent maximum anodic currents exhibited a noticeable deviation from the exponential relationship at 90 °C. At room temperature the short term (2 to 20 hours) apparent maximum anodic currents of the freshly polished electrodes were about 6×10^{-8} A/cm^2 for alloy 22, and from 3×10^{-4} to 1×10^{-3} A/cm^2 for types 304 and 316 stainless steels and alloy 600 under the test conditions. As temperature increased from 18 to 90°C, they all increased by a factor of approximately 50.

The regression parameters for the dependence of the apparent maximum current density on the reciprocal of temperature and the activation energies are shown in Table 3. The temperature ranges for the regression are 18 to 60°C for alloy 22 and 18 to 90°C for the others. The activation energies are approximately 45kJ/mol for the types 304 and 316 stainless steels and approximately 23 kJ/mol for alloys 22 and 600.

Figure 14 presents the comparison of the maximum anodic current densities obtained in several experiments for the different metals in three solutions at the end of the exposures. As shown in Figure 14, the order of increasing corrosivity of the solutions tested is as follows:

$$\text{DI Water} < 0.5\text{M NaCl} < 0.1\text{ M } FeCl_3$$

The resistance of the alloys in all solutions increases in the same order, i.e.:

$$\text{Carbon Steel} < \text{alloy 600} < \text{type 304} < \text{type 316} < \text{alloy 276} < \text{alloy 22}$$

This order is also consistent with the pitting resistance equivalent numbers calculated according to the elemental composition of the alloys[18] (Table 2).

Figure 15 also shows that the sensor's detection limit for the maximum anodic current density with 1 mm diameter electrodes is 2×10^{-8} A/cm^2. The maximum anodic currents for alloy 22 at the end of exposures in all solutions are close or below the detection limit of the sensor.

CONCLUSIONS

A galvanically coupled multiple-electrode sensor was used to measure the real-time localized corrosion of Fe-Ni-Cr-Mo alloys in chloride solutions. It was demonstrated that the localized corrosion sensor provided a rapid real-time response to the changes in temperature and salt concentration and has a detection limit of 5×10^{-11} A with respect to corrosion currents and 2×10^{-8} A/cm^2 with respect to apparent maximum anodic current density for the miniature electrodes used in the sensors. At room temperature, the sensor is adequately sensitive for localized corrosion of types 304 and 316 stainless steel, alloy 600 and alloy 276 in de-ionized water. The alloy 22 was found to be the most resistant to localized corrosion among the alloys tested. Work is in progress to calculate the penetration rate from the measured current densities.

ACKNOWLEDGEMENTS

The authors would like to thank J. Aaron for assistance in the experiment, C.S. Brossia, O.C. Moghissi and D.S. Dunn for technical discussions, and the Advisory Committee for Research of the Southwest Research Institute for providing the funding for this work. The paper is an independent product of the Center for Nuclear Waste Regulatory Analyses and does not necessarily reflect the views or the regulatory position of the US Nuclear Regulatory Commission.

REFERENCES

1. Civilian Radioactive Waste Management System Management and Operating Contractor, "General Corrosion and Localized Corrosion of Waste Package Outer Barrier", Civilian Waste

Management System Management and Contractor, Las Vegas, N.V., ANL-EBS-MD-000003, Revision 00, 2000.

2. Civilian Radioactive Waste Management System Management and Operating Contractor, "Repository Safety Strategy: Plan to Prepare the Postclosure Safety Case to Support Yucca Mountain Site Recommendation and Licensing Considerations" Civilian Waste Management System Management and Contractor, Las Vegas, N.V., TDR-WIS/RL-000001, Revision 3, 2000.

3. N. Sridhar, D.S. Dunn, C.S. Brossia, and G.A. Cragnolino, "Stabilization and Repassivation of Localized Corrosion," in Research Topical Symposium, G.S. Frankel and J.R. Scully (Eds.), (Houston, TX: NACE International, 2001), pp.1-29.

4. L. Yang, X. Sun, and F. Steward, "An Electrical Resistance Probe for Monitoring Flow Assisted Corrosion in Simulated Primary Coolant of Nuclear Reactors at 310°C", CORROSION/99, paper no. 459, (Houston, TX: NACE International, 1999).

5. G.K. Brown, J.R. Davies, and B.J. Hemblade, "Real Time Metal Loss Internal Monitoring", CORROSION/2000, paper no. 278, (Houston, TX: NACE International, 2000).

6. N. Sridhar, D.S. Dunn, C.S. Brossia, and O.C. Moghissi, "Corrosion Monitoring Techniques for Thermally Driven Wet and Dry Conditions", CORROSION/2000, paper no. 283, (Houston, TX: NACE International, 2000).

7. F. Mansfeld, "The Polarization Resistance Technique for Measuring Corrosion Currents," in Advances in Corrosion Engineering and Technology, M. G. Fontana and R.W. Staehle (Eds.), Vol. 6, (New York: Plenum, 1976), Chapter 3.

8. F. Mansfeld, "Polarization Resistance Measurements-Today's Status," in Electrochemical Techniques for Corrosion Engineering, R. Baboian (Ed.), (Houston, TX: NACE International, 1987).

9. A. N. Rothwell, D.A. Eden, and G. Row, "Electrochemical Noise Techniques for Determining Corrosion Rates and Mechanisms", CORROSION/92, paper no. 223 (Houston, TX: NACE International, 1992).

10. J.A. Wharton, B. G. Mellor, R.J.K. Wood, and C.J. Smith, Journal of Electrochemical Society 147, 9(2000), p.3294.

11 R.G. Kelly, M.E. Inman, and J.L. Hudson, "Analysis of Electrochemical Noise for type 410 Stainless Steel in Chloride Solutions," in Electrochemical Noise Measurement for Corrosion Applications, J.R. Kearns, J.R. Scully, P.R. Roberge, D.L. Reichert, and J.L. Dawson (Eds.), (Conshohocken, PA: American Society for Testing and Materials, Special Technical Publication 1277, 1996), p. 101.

12. S.T. Pride, J. R. Scully, and J.L. Hudson, "Analysis of Electrochemical Noise from Metastable Pitting in Aluminum, Aged Al-2%Cu, and AA 2024-T3," in Electrochemical Noise Measurement for Corrosion Applications, J.R. Kearns, J.R. Scully, P.R. Roberge, D.L. Reichert, and J.L. Dawson, (Eds.), (Conshohocken, PA: American Society for Testing and Materials, Special Technical Publication 1277, 1996), p. 307.

13. L. Yang, N. Sridhar, and O. Pensado, "Development of a Multi-Electrode Array Sensor for Monitoring Localized Corrosion," presented at the 199th Meeting of the Electrochemical Society, Abstract #182, Extended Abstract Volume I, Washington DC, 2001.

14. Y. J. Tan, "Wire Beam Electrode: A New Tool for Studying Localized Corrosion and Other Inheterogeinity Electrochemical Processes", Corrosion Science 41, (1999), p.226.

15. Y. J. Tan, S. Bailey, B. Kinsella, and A. Lowe, "Mapping Corrosion Kinetics Using the Wire Beam Electrode in Conjunction with Electrochemical Noise Resistance Measurements", Journal of Electrochemical Society 147, 2 (2000), p.530.

16. L. Yang, N. Sridhar, O. Pensado, and D. Dunn, "An In-situ Galvanically Coupled Multielectrode Array Sensor for Localized Corrosion", submitted to Corrosion (2002)

17. L. Yang, and D. Dunn, "Evaluation of Corrosion Inhibitors in Cooling Water Systems Using a Coupled Multielectrode Array Sensor" CORROSION/2002, paper no. 02004, (Houston, TX: NACE International, 2002).

18. R.B. Rebak, and P. Crook, "Improved Pitting and Crevice Corrosion Resistance of Nickel and Cobalt Based Alloys," in Proceedings of the Symposium on Critical Factors in Localized Corrosion III, R.G. Kelly, G.S. Frankel, P.M. Natishan and R.C. Newman (Eds.), (Pennington, NJ: Electrochemical Society, 1999), pp.289-302.

Table 1 Chemical compositions (%wt) of the metal wires used in the sensors

Metals	UNS #	Ni	Cr	Fe	Mo	Mn	W	Co	Si (ppm)	C (ppm)
Type 304	S30400	9.5	18.5	Bal	Na	<2	Na	Na	Na	<800
Type 316	S31600	11	17.7	Bal	3	<2	Na	Na	Na	<1200
Alloy 22	N06022	Bal	20.5	4.9	15.1	0.29	2.75	0.6	400	180
Alloy 276	N10276	Bal	15.4	6.1	15.48	0.4	3.6	0.73	540	60
Alloy 600	N06600	Bal	15.5	8	Na	Na	Na	Na	Na	<1500

Na-Not available; Bal- Balance

Table 2 Pitting resistance equivalent numbers calculated according to the elemental composition of the alloys[18]:

PRE Numbers	N06022	N10276	S31600	S30400	N06600
PRE (Eq. 1)	70.3	66.5	27.6	18.5	15.5
PRE' (Eq. 2)	79.4	78.4	27.6	18.5	15.5
PRE" (Eq. 3)	59.3	55.8	24.9	19.7	17.1

Table 3. Regression parameters of the dependence of the apparent maximum anodic current densities on temperature, $i_{max}= i_o exp(-k/T)$, and the activation energies for the different sensors*.

Sensors	i_o (A/cm^2)	K (K)	R^2	E (kJ/mol)
Type 304	2.03×10^5	-5936	0.996	49.4
Type 316	7.25	-5051	0.912	42.0
Alloy 600	29.8	-2913	0.925	24.2
Alloy 22	6.55×10^{-4}	-2707	0.999	22.5

* Temperature ranges are 18-60°C for alloy 22 and 18-90°C for all other sensors

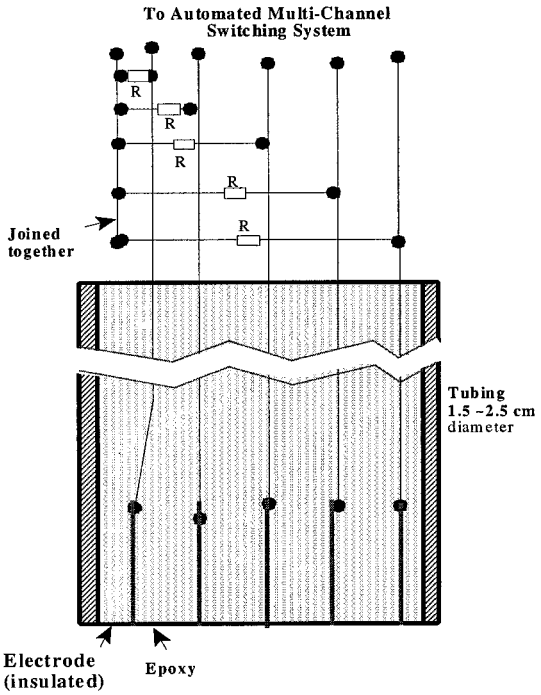

Figure 1 Schematic diagram of the coupled multiple-electrode array sensor for localized corrosion.

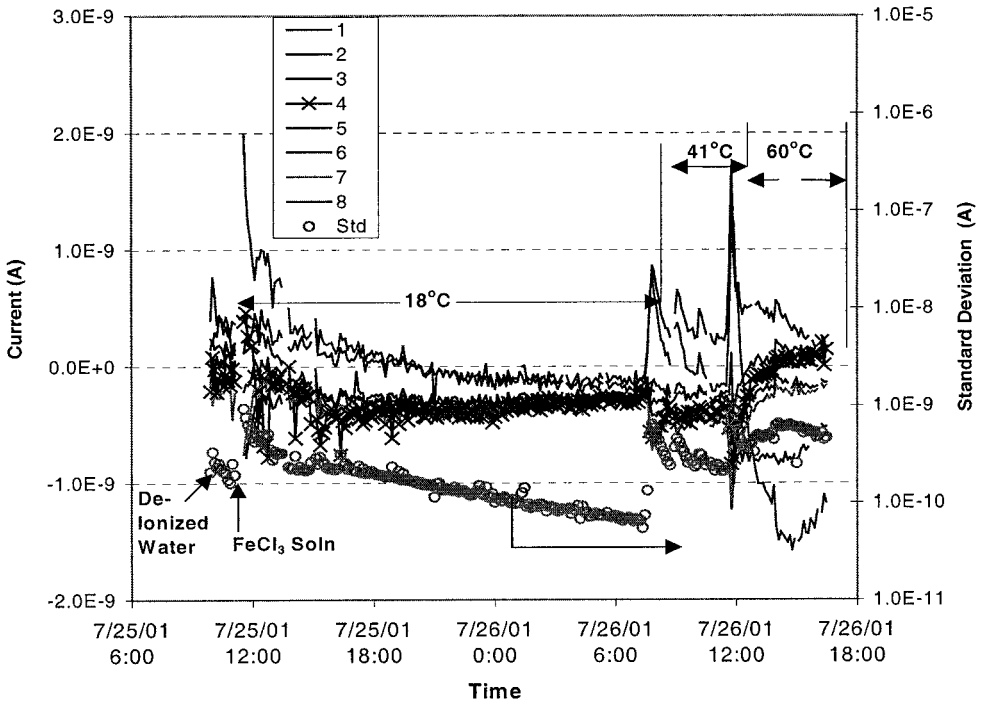

Figure 2 The response of the currents of an eight-electrode alloy 22 sensor and its standard deviation to the changes in temperature in 0.1 M ferric chloride solution.
Note: The numbers in the legend are the electrode numbers in the sensor.

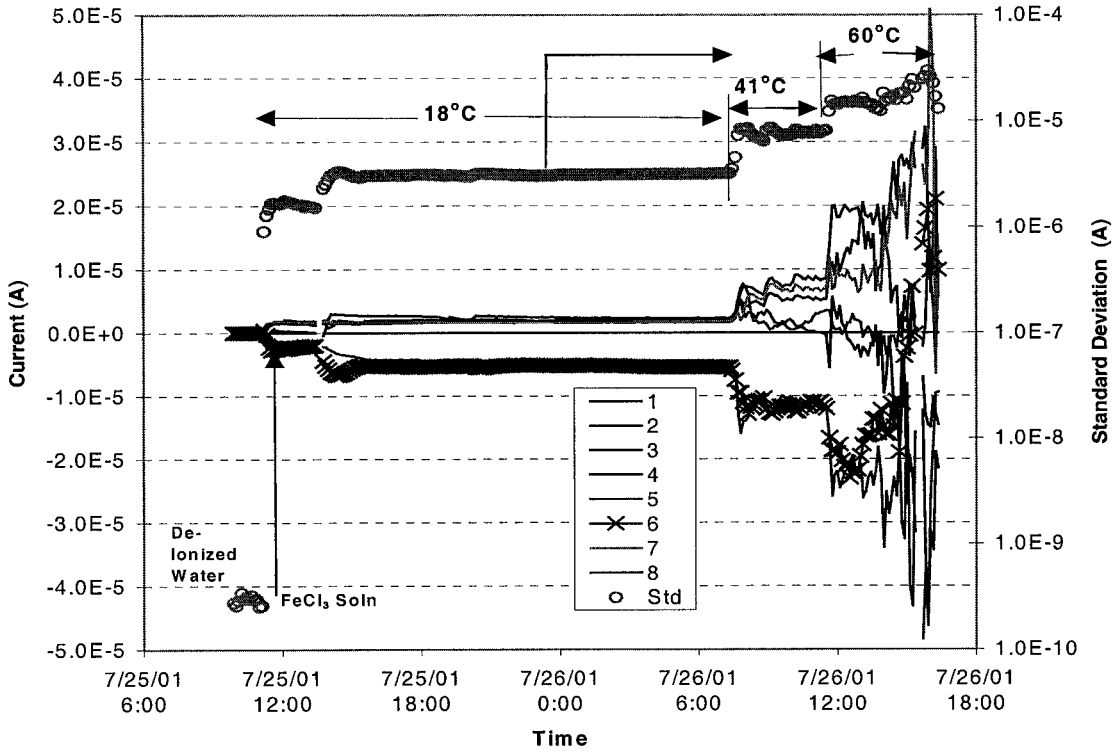

Figure 3 The response of the currents of an eight-electrode alloy 600 alloy sensor and its standard deviation to the changes in temperature in 0.1 M ferric chloride solution.

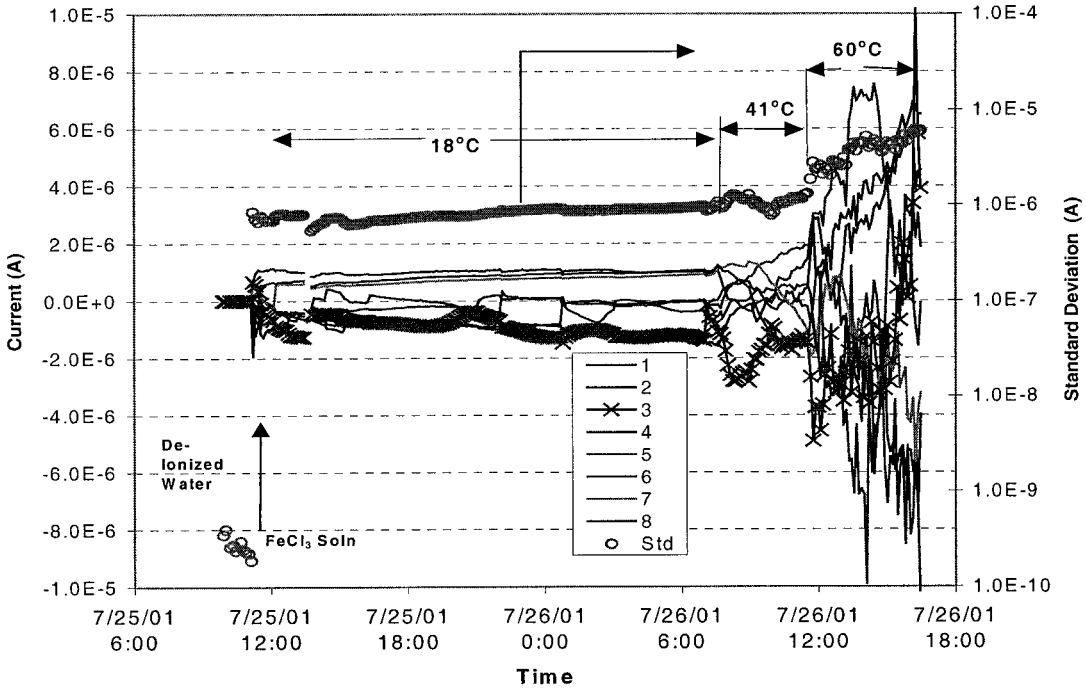

Figure 4 The response of the currents of an eight-electrode type 316 stainless steel sensor and its standard deviation to the changes in temperature in 0.1 M ferric chloride solution.

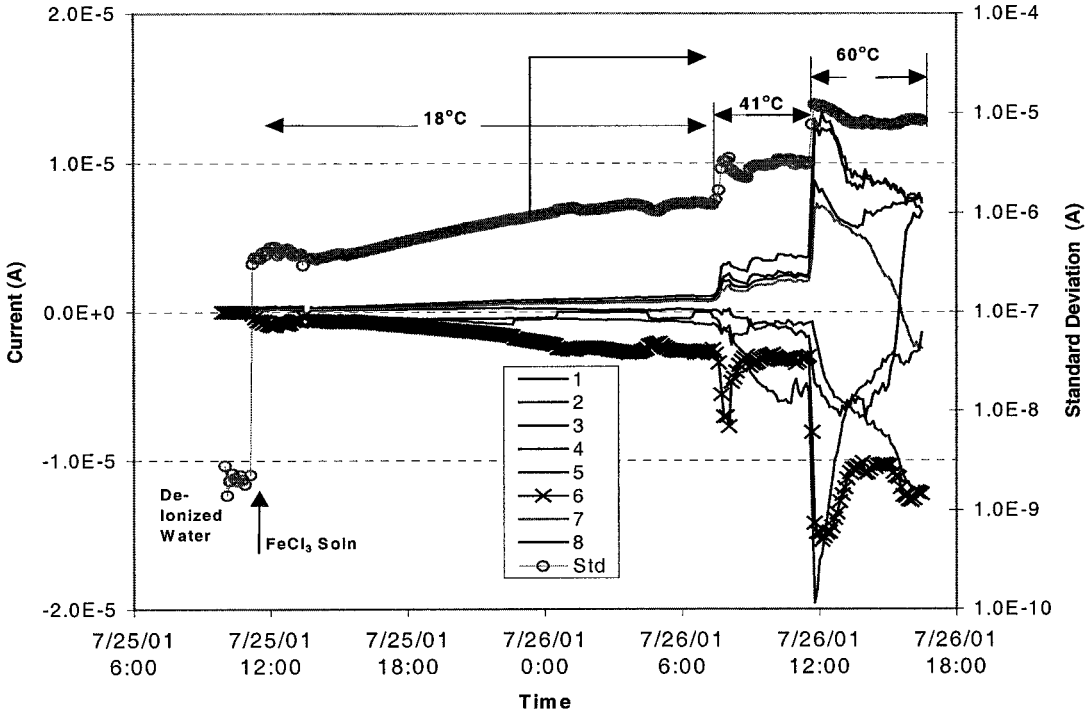

Figure 5 The response of the currents of an eight-electrode type 304 stainless steel sensor and its standard deviation to the changes in temperature in 0.1 M ferric chloride solution.
Note: The numbers in the legend are the electrode numbers in the sensor.

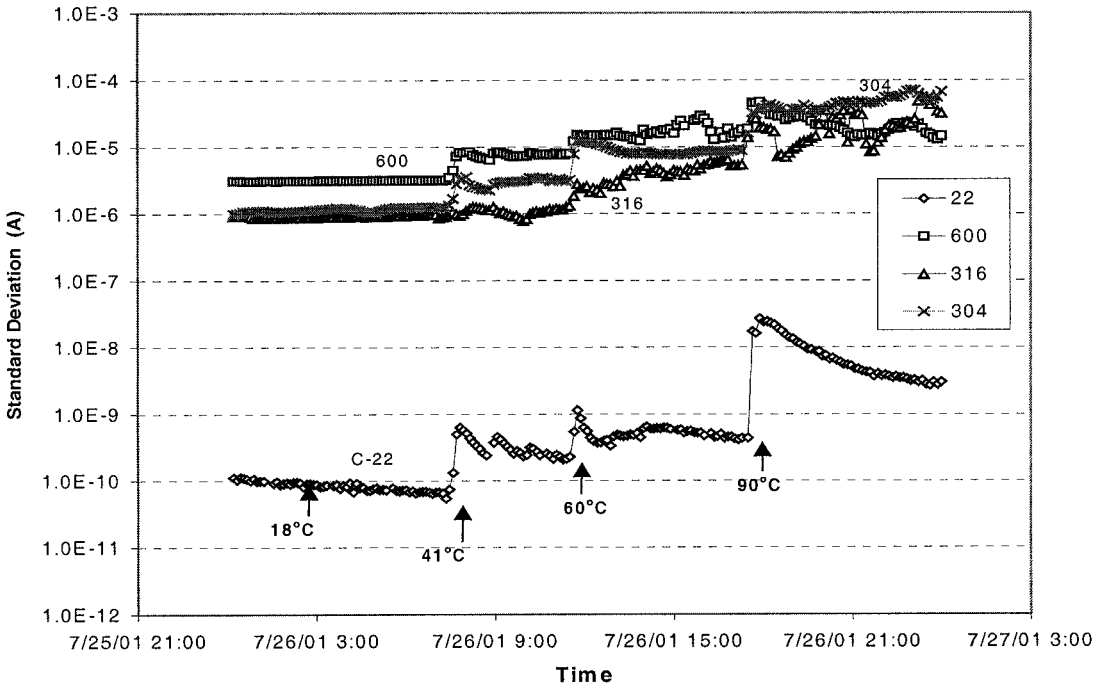

Figure 6 Comparison of the standard deviation signals of four different sensors in 0.1 M ferric chloride solution at different temperatures.

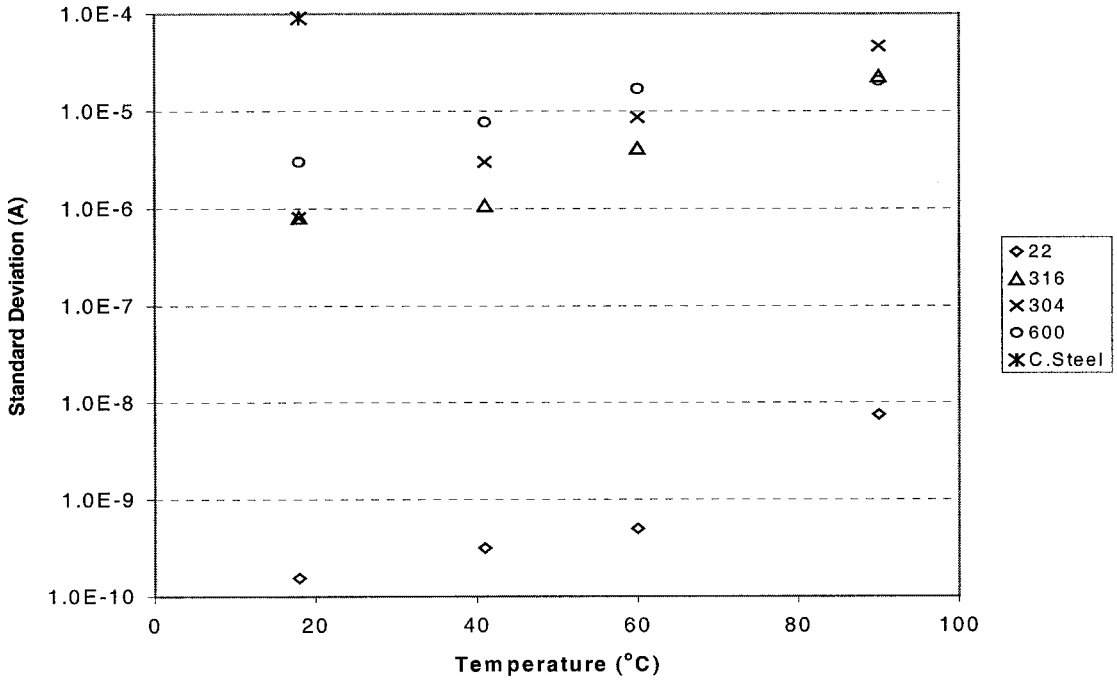

Figure 7 Relationship between the standard deviation signals of five different sensors in 0.1 M ferric chloride solution and temperature.

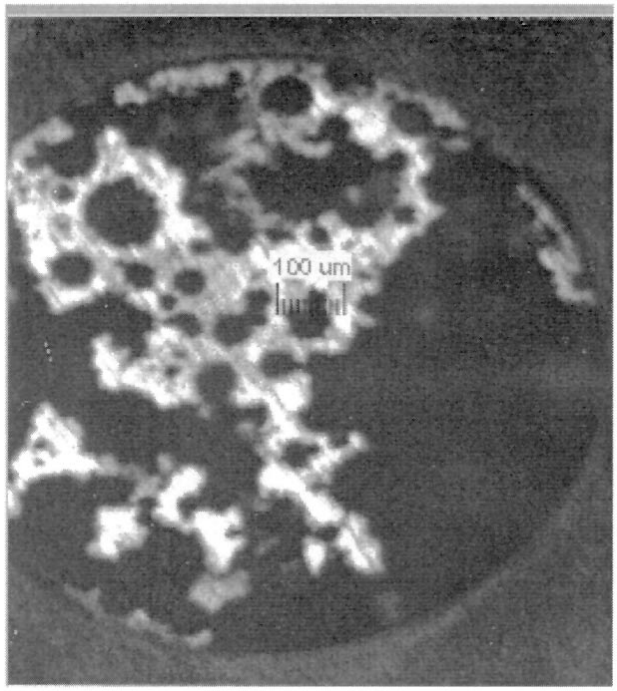

Figure 8 Post test examination of the surface of an electrode in the type 304 stainless steel sensor.

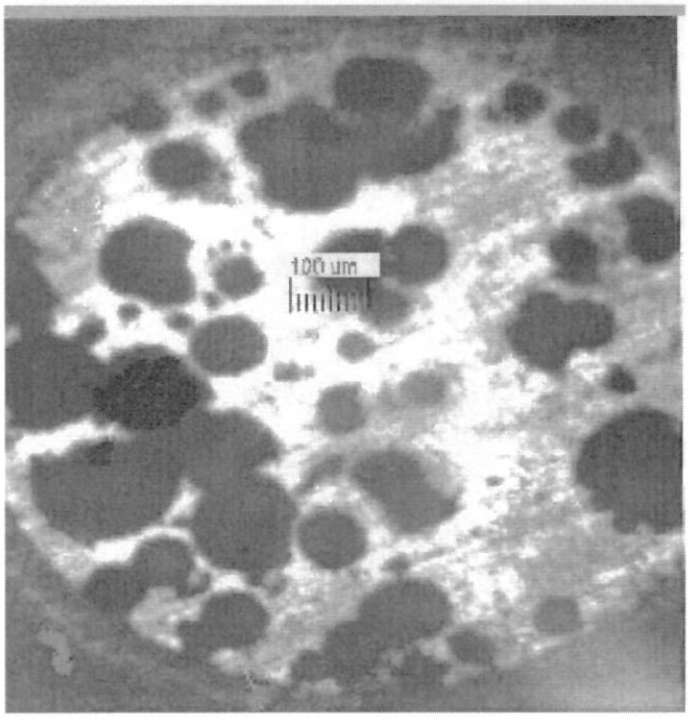

Figure 9 Post test examination of the surface of an electrode in the type 316 stainless steel sensor.

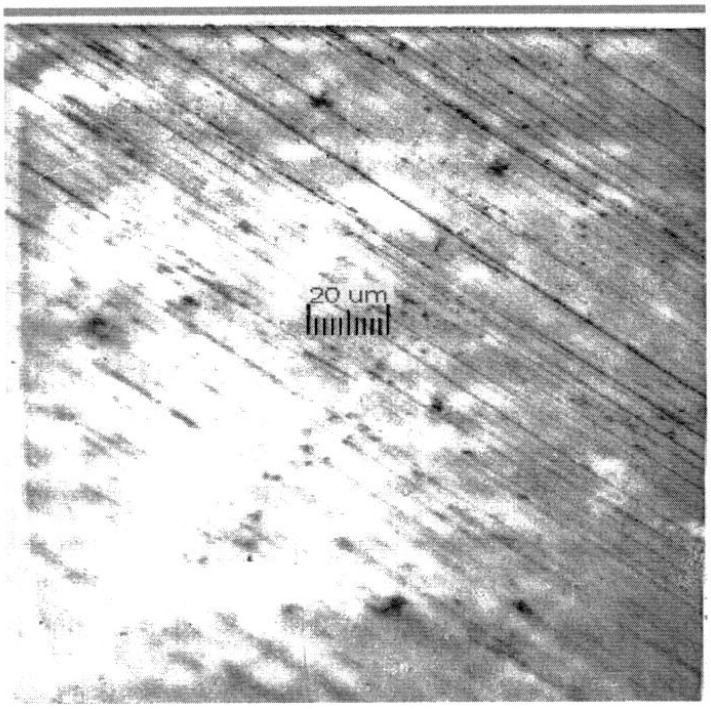

Figure 10 Post test examination of the surface of an electrode in the alloy 22 sensor.

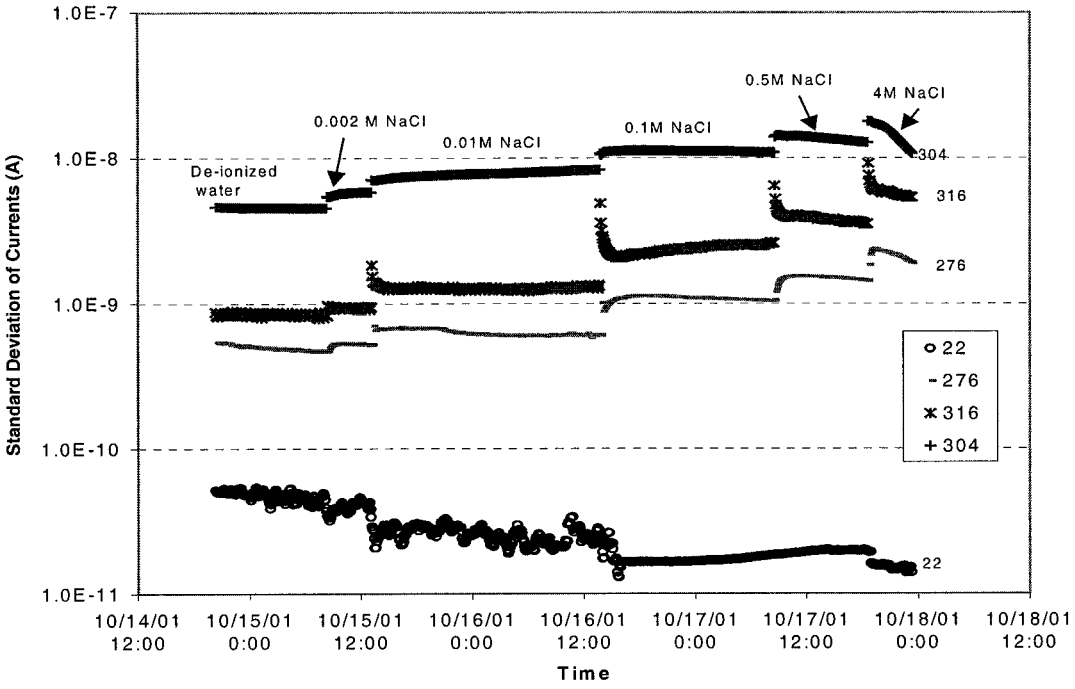

Figure 11 Responses of the standard deviations of four sensors (types 304 and 316 stainless steels and alloys 276 and 22) to the changes in chloride concentration at room temperature.

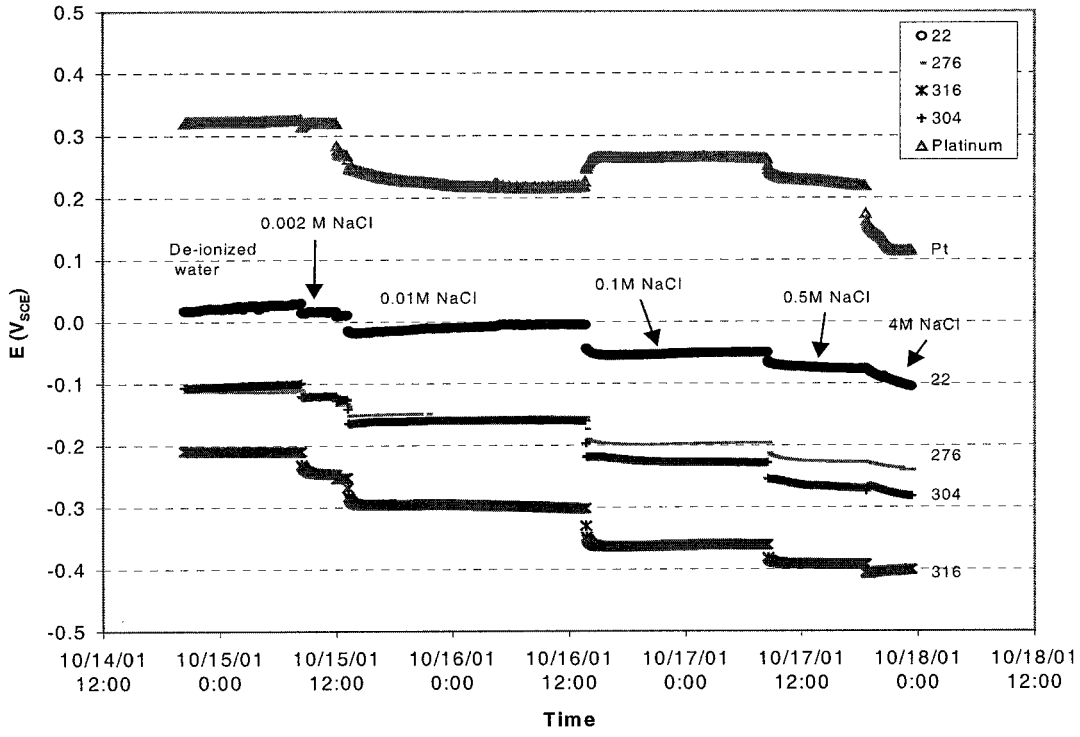

Figure 12 Responses of the open circuit potentials of a platinum electrode and four sensors (types 304 and 316 stainless steels and alloys 276 and 22) to the changes in chloride concentration at room temperature.

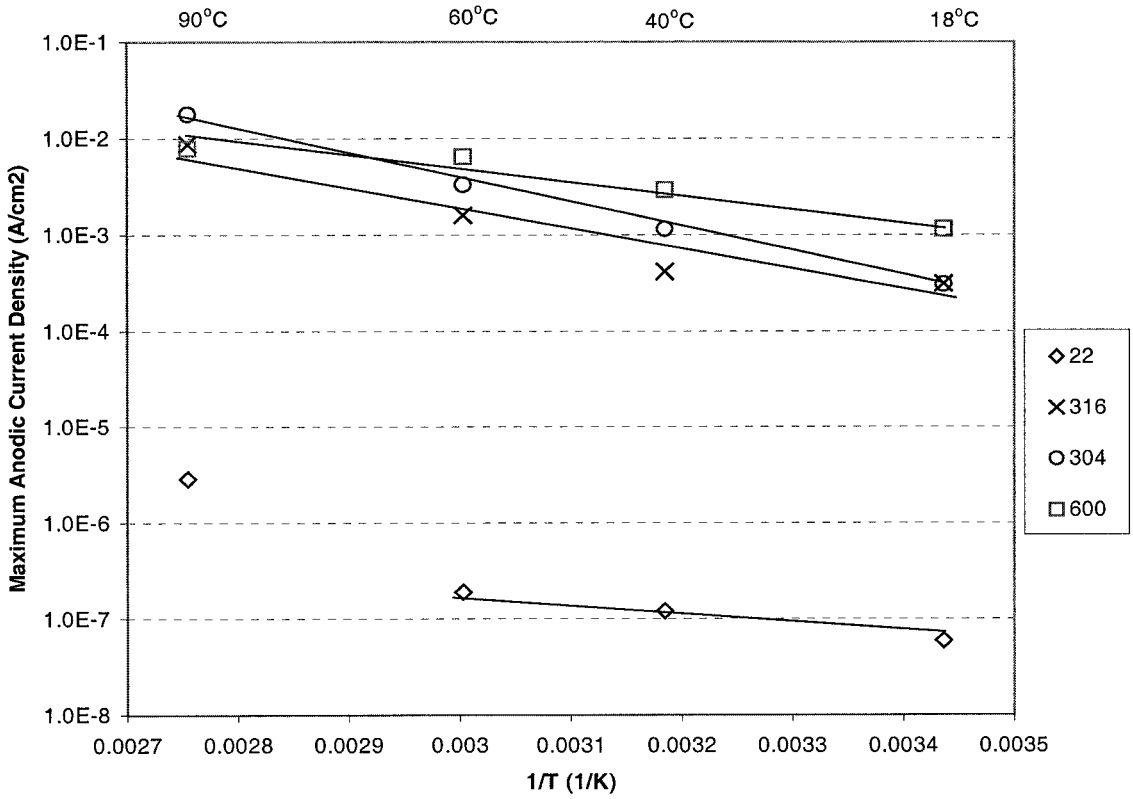

Figure 13 Apparent maximum anodic current of different sensors as a function of the reciprocal of temperature in the $FeCl_3$ solution.

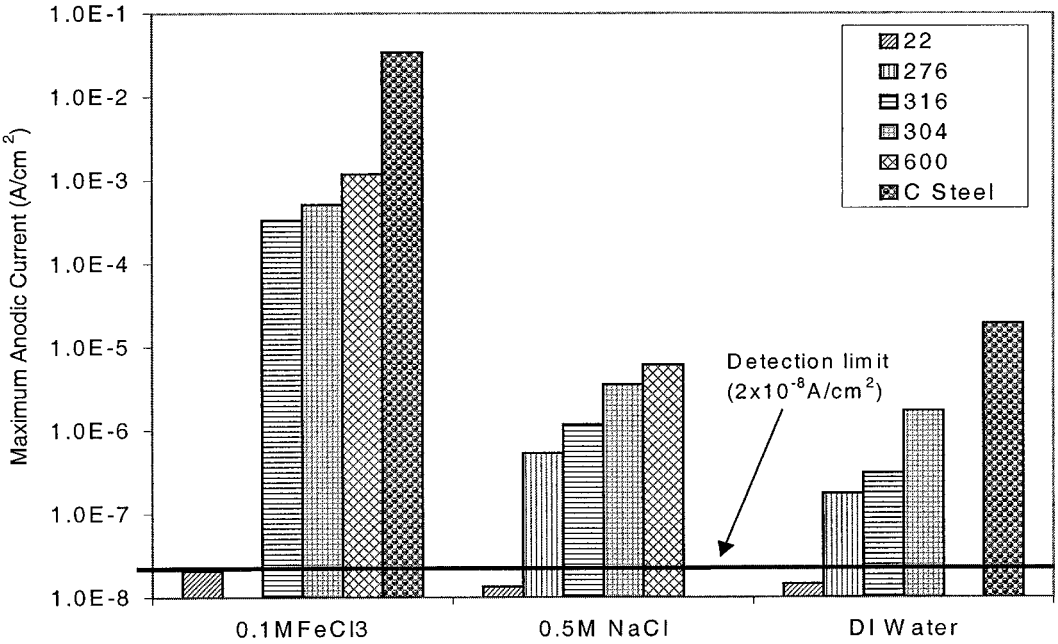

Figure 14 Apparent maximum anodic current densities in different solutions at the end of exposures for the various freshly polished metals.